Search for a Scalar Top almost degenerate with the lightest Neutralino in e^+e^- collisions at $\sqrt{s}$ up to 202 GeV

R. Barate, D. Decamp, P. Ghez, C. Goy, S. Jezequel, J P. Lees, F. Martin, E. Merle, M N. Minard, B. Pietrzyk, et al.

HAL Id: in2p3-00005671
https://hal.in2p3.fr/in2p3-00005671

Submitted on 15 Sep 2000

Search for a Scalar Top almost degenerate with the lightest Neutralino in e^+e^- Collisions at $\sqrt{s}$ up to 202 GeV

The ALEPH Collaboration[*])

Abstract

Data collected at centre-of-mass energies from 189 GeV to 202 GeV by the ALEPH detector at LEP, corresponding to an integrated luminosity of 411 pb^{-1}, are analysed in a search for the scalar top in the decay channels $\tilde{t} \to c/u\,\chi$ for small mass differences between the stop and the lightest neutralino. No evidence for deviations from the Standard Model expectation is found and a lower limit of 59 GeV/c^2 is set for the stop mass, independent of the stop to neutralino mass difference and of the stop lifetime.

(Submitted to Physics Letters B)

---

[*]) See following pages for the list of authors

The ALEPH Collaboration

R. Barate, D. Decamp, P. Ghez, C. Goy, S. Jezequel, J.-P. Lees, F. Martin, E. Merle, M.-N. Minard, B. Pietrzyk

  Laboratoire de Physique des Particules (LAPP), IN²P³-CNRS, F-74019 Annecy-le-Vieux Cedex, France

S. Bravo, M.P. Casado, M. Chmeissani, J.M. Crespo, E. Fernandez, M. Fernandez-Bosman, Ll. Garrido,[15]
E. Graugés, J. Lopez, M. Martinez, G. Merino, R. Miquel, Ll.M. Mir, A. Pacheco, D. Paneque, H. Ruiz

  Institut de Física d'Altes Energies, Universitat Autònoma de Barcelona, E-08193 Bellaterra (Barcelona), Spain[7]

A. Colaleo, D. Creanza, N. De Filippis, M. de Palma, G. Iaselli, G. Maggi, M. Maggi, S. Nuzzo, A. Ranieri,
G. Raso,[24] F. Ruggieri, G. Selvaggi, L. Silvestris, P. Tempesta, A. Tricomi,[3] G. Zito

  Dipartimento di Fisica, INFN Sezione di Bari, I-70126 Bari, Italy

X. Huang, J. Lin, Q. Ouyang, T. Wang, Y. Xie, R. Xu, S. Xue, J. Zhang, L. Zhang, W. Zhao

  Institute of High Energy Physics, Academia Sinica, Beijing, The People's Republic of China[8]

D. Abbaneo, G. Boix,[6] O. Buchmüller, M. Cattaneo, F. Cerutti, G. Dissertori, H. Drevermann, R.W. Forty,
M. Frank, F. Gianotti, T.C. Greening, J.B. Hansen, J. Harvey, P. Janot, B. Jost, M. Kado, V. Lemaitre,
P. Maley, P. Mato, A. Minten, A. Moutoussi, F. Ranjard, L. Rolandi, D. Schlatter, M. Schmitt,[20] O. Schneider,[2]
P. Spagnolo, W. Tejessy, F. Teubert, E. Tournefier, A. Valassi, J.J. Ward, A.E. Wright

  European Laboratory for Particle Physics (CERN), CH-1211 Geneva 23, Switzerland

Z. Ajaltouni, F. Badaud, G. Chazelle, O. Deschamps, S. Dessagne, A. Falvard, P. Gay, C. Guicheney, P. Henrard,
J. Jousset, B. Michel, S. Monteil, J-C. Montret, D. Pallin, J.M. Pascolo, P. Perret, F. Podlyski

  Laboratoire de Physique Corpusculaire, Université Blaise Pascal, IN²P³-CNRS, Clermont-Ferrand, F-63177 Aubière, France

J.D. Hansen, J.R. Hansen, P.H. Hansen,[1] B.S. Nilsson, A. Wäänänen

  Niels Bohr Institute, 2100 Copenhagen, DK-Denmark[9]

G. Daskalakis, A. Kyriakis, C. Markou, E. Simopoulou, A. Vayaki

  Nuclear Research Center Demokritos (NRCD), GR-15310 Attiki, Greece

A. Blondel,[12] J.-C. Brient, F. Machefert, A. Rougé, M. Swynghedauw, R. Tanaka
H. Videau

  Laboratoire de Physique Nucléaire et des Hautes Energies, Ecole Polytechnique, IN²P³-CNRS, F-91128 Palaiseau Cedex, France

E. Focardi, G. Parrini, K. Zachariadou

  Dipartimento di Fisica, Università di Firenze, INFN Sezione di Firenze, I-50125 Firenze, Italy

A. Antonelli, M. Antonelli, G. Bencivenni, G. Bologna,[4] F. Bossi, P. Campana, G. Capon, V. Chiarella,
P. Laurelli, G. Mannocchi,[5] F. Murtas, G.P. Murtas, L. Passalacqua, M. Pepe-Altarelli

  Laboratori Nazionali dell'INFN (LNF-INFN), I-00044 Frascati, Italy

M. Chalmers, A.W. Halley, J. Kennedy, J.G. Lynch, P. Negus, V. O'Shea, B. Raeven, D. Smith, P. Teixeira-Dias,
A.S. Thompson

  Department of Physics and Astronomy, University of Glasgow, Glasgow G12 8QQ,United Kingdom[10]

R. Cavanaugh, S. Dhamotharan, C. Geweniger,[1] P. Hanke, V. Hepp, E.E. Kluge, G. Leibenguth, A. Putzer,
K. Tittel, S. Werner,[19] M. Wunsch[19]

  Kirchhoff-Institut für Physik, Universität Heidelberg, D-69120 Heidelberg, Germany[16]

R. Beuselinck, D.M. Binnie, W. Cameron, G. Davies, P.J. Dornan, M. Girone, N. Marinelli, J. Nowell, H. Przysiezniak,[1] J.K. Sedgbeer, J.C. Thompson,[14] E. Thomson,[23] R. White

Department of Physics, Imperial College, London SW7 2BZ, United Kingdom[10]

V.M. Ghete, P. Girtler, E. Kneringer, D. Kuhn, G. Rudolph

Institut für Experimentalphysik, Universität Innsbruck, A-6020 Innsbruck, Austria[18]

C.K. Bowdery, P.G. Buck, D.P. Clarke, G. Ellis, A.J. Finch, F. Foster, G. Hughes, R.W.L. Jones, N.A. Robertson, M. Smizanska

Department of Physics, University of Lancaster, Lancaster LA1 4YB, United Kingdom[10]

I. Giehl, F. Hölldorfer, K. Jakobs, K. Kleinknecht, M. Kröcker, A.-S. Müller, H.-A. Nürnberger, G. Quast,[1] B. Renk, E. Rohne, H.-G. Sander, S. Schmeling, H. Wachsmuth, C. Zeitnitz, T. Ziegler

Institut für Physik, Universität Mainz, D-55099 Mainz, Germany[16]

A. Bonissent, J. Carr, P. Coyle, C. Curtil, A. Ealet, D. Fouchez, O. Leroy, T. Kachelhoffer, P. Payre, D. Rousseau, A. Tilquin

Centre de Physique des Particules de Marseille, Univ Méditerranée, IN^{2}P^3-CNRS, F-13288 Marseille, France

M. Aleppo, S. Gilardoni, F. Ragusa

Dipartimento di Fisica, Università di Milano e INFN Sezione di Milano, I-20133 Milano, Italy.

H. Dietl, G. Ganis, A. Heister, K. Hüttmann, G. Lütjens, C. Mannert, W. Männer, H.-G. Moser, S. Schael, R. Settles,[1] H. Stenzel, W. Wiedenmann, G. Wolf

Max-Planck-Institut für Physik, Werner-Heisenberg-Institut, D-80805 München, Germany[16]

P. Azzurri, J. Boucrot,[1] O. Callot, M. Davier, L. Duflot, J.-F. Grivaz, Ph. Heusse, A. Jacholkowska,[1] L. Serin, J.-J. Veillet, I. Videau,[1] J.-B. de Vivie de Régie, D. Zerwas

Laboratoire de l'Accélérateur Linéaire, Université de Paris-Sud, IN^{2}P^3-CNRS, F-91898 Orsay Cedex, France

G. Bagliesi, T. Boccali, G. Calderini, V. Ciulli, L. Foà, A. Giammanco, A. Giassi, F. Ligabue, A. Messineo, F. Palla,[1] G. Rizzo, G. Sanguinetti, A. Sciabà, G. Sguazzoni, R. Tenchini,[1] A. Venturi, P.G. Verdini

Dipartimento di Fisica dell'Università, INFN Sezione di Pisa, e Scuola Normale Superiore, I-56010 Pisa, Italy

G.A. Blair, J. Coles, G. Cowan, M.G. Green, D.E. Hutchcroft, L.T. Jones, T. Medcalf, J.A. Strong, J.H. von Wimmersperg-Toeller

Department of Physics, Royal Holloway & Bedford New College, University of London, Surrey TW20 OEX, United Kingdom[10]

R.W. Clifft, T.R. Edgecock, P.R. Norton, I.R. Tomalin

Particle Physics Dept., Rutherford Appleton Laboratory, Chilton, Didcot, Oxon OX11 OQX, United Kingdom[10]

B. Bloch-Devaux, D. Boumediene, P. Colas, B. Fabbro, G. Faïf, E. Lançon, M.-C. Lemaire, E. Locci, P. Perez, J. Rander, J.-F. Renardy, A. Rosowsky, P. Seager,[13] A. Trabelsi,[21] B. Tuchming, B. Vallage

CEA, DAPNIA/Service de Physique des Particules, CE-Saclay, F-91191 Gif-sur-Yvette Cedex, France[17]

S.N. Black, J.H. Dann, C. Loomis, H.Y. Kim, N. Konstantinidis, A.M. Litke, M.A. McNeil, G. Taylor

Institute for Particle Physics, University of California at Santa Cruz, Santa Cruz, CA 95064, USA[22]

C.N. Booth, S. Cartwright, F. Combley, P.N. Hodgson, M. Lehto, L.F. Thompson

Department of Physics, University of Sheffield, Sheffield S3 7RH, United Kingdom[10]

K. Affholderbach, A. Böhrer, S. Brandt, C. Grupen,[1] J. Hess, A. Misiejuk, G. Prange, U. Sieler

Fachbereich Physik, Universität Siegen, D-57068 Siegen, Germany[16]

C. Borean, G. Giannini, B. Gobbo

Dipartimento di Fisica, Università di Trieste e INFN Sezione di Trieste, I-34127 Trieste, Italy

H. He, J. Putz, J. Rothberg, S. Wasserbaech

Experimental Elementary Particle Physics, University of Washington, Seattle, WA 98195 U.S.A.

S.R. Armstrong, K. Cranmer, P. Elmer, D.P.S. Ferguson, Y. Gao, S. González, O.J. Hayes, H. Hu, S. Jin, J. Kile, P.A. McNamara III, J. Nielsen, W. Orejudos, Y.B. Pan, Y. Saadi, I.J. Scott, J. Walsh, J. Wu, Sau Lan Wu, X. Wu, G. Zobernig

Department of Physics, University of Wisconsin, Madison, WI 53706, USA[11]

1   Introduction

In the Minimal Supersymmetric extension of the Standard Model (MSSM), each chirality state of the Standard Model fermions has a scalar supersymmetric partner. The partners $\tilde{t}_R$ and $\tilde{t}_L$ of the right and left-handed states of the top quark are weak interaction eigenstates which mix to form mass eigenstates. The mixing angle $\theta_{\tilde{t}}$ is defined such that the lighter of the mass eigenstates, the stop, is given by $\tilde{t} = \tilde{t}_L \cos\theta_{\tilde{t}} + \tilde{t}_R \sin\theta_{\tilde{t}}$. Since the off-diagonal terms of the mixing matrix are proportional to the mass of the Standard Model partner, the stop could well be the lightest scalar quark, and even the lightest supersymmetric charged particle [1], hence the interest in searches for stop pair-production in e^+e^- collisions at LEP energies [2].

In this letter, it is assumed that all supersymmetric particles except the lightest neutralino χ are heavier than the stop, and that R-parity is conserved. It is furthermore assumed that there is no source of flavour changing neutral currents in the MSSM in addition to those already present in the Standard Model. Under those assumptions, the dominant stop decay mode is $\tilde{t} \to c\chi$, if kinematically allowed. This process is mediated only by loop diagrams, with a width which can be parametrized as [3]

$$\Gamma_{\tilde{t} \to c\chi} = (0.3 \div 3) \times 10^{-10} \times m_{\tilde{t}} \left(1 - \frac{m_\chi^2}{m_{\tilde{t}}^2}\right)^2 .$$

This decay width depends on the mass difference Δm between the stop and the neutralino, and on the masses and field content of the particles involved in the loops. For low enough Δm values, the stop lifetime becomes sizeable, and has to be taken into account in the searches for stop production. If Δm is so small that the $\tilde{t} \to c\chi$ channel is kinematically closed, the dominant decay mode becomes $\tilde{t} \to u\chi$, and the stop can then be considered as stable for practical purposes. The stop decay length as a function of $m_{\tilde{t}}$ and Δm is shown in Fig. 1 in the case of pair production in e^+e^- collisions at $\sqrt{s} = 189\,\text{GeV}$. (For the purpose of this figure, $\theta_{\tilde{t}} = 56°$, $\mu = -100$ GeV and $\tan\beta = 1.5$ have been assumed, where μ is the supersymmetric Higgs mass term, and $\tan\beta$ is the ratio of the vacuum expectation values of the two Higgs doublets.)

The searches for a scalar top performed up to now by ALEPH [4, 5, 6, 7] are valid under the assumption of a negligible stop lifetime. This assumption is justified for $\Delta m \gtrsim 6$ GeV/c^2, in which case a stop mass lower limit of 87 GeV/c^2 has been obtained [7]. In this letter, smaller stop to neutralino mass differences are specifically addressed, with the effects of the finite stop lifetime explicitly taken into account. Dedicated topological selections have been designed to cope with the peculiar phenomenology of the very small Δm regime. Together with the already existing selections, they were applied to the data collected at centre-of-mass energies ranging from 189 to 202 GeV, corresponding to a total integrated luminosity of 411 pb^{-1}. As a result, a stop mass lower limit is obtained, independent of the stop to neutralino mass difference and of the stop lifetime.
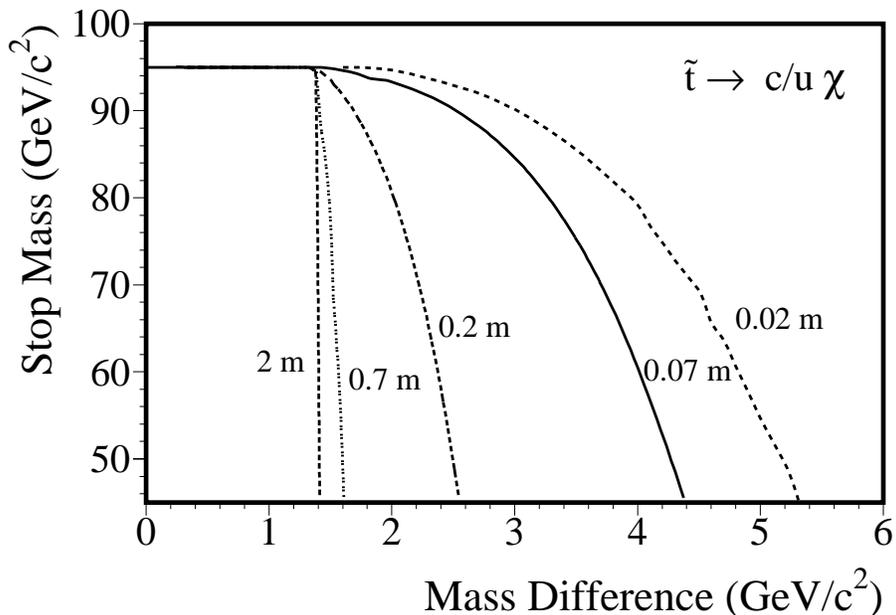
1

Figure 1: The decay length of a stop produced at $\sqrt{s} = 189\,\mathrm{GeV}$ as a function of Δm and $m_{\tilde{t}}$, calculated in the MSSM for $\theta_{\tilde{t}} = 56°$, $\mu = -100$ GeV and $\tan\beta = 1.5$.

2 The ALEPH detector

A detailed description of the ALEPH detector is given in Ref. [8], and an account of its performance as well as a description of the reconstruction algorithms can be found in Ref. [9]. Only a brief description of the detector components and algorithms relevant for this analysis is given here.

The trajectories of charged particles are measured by a silicon vertex detector (VDET), a cylindrical multi-wire drift chamber (ITC) and a large time projection chamber (TPC). These detectors are immersed in an axial magnetic field of 1.5 T provided by a superconducting solenoidal coil, and the transverse momentum resolution achieved is $\sigma(p_T)/p_T = 0.0006\ p_T \oplus$ 0.005 (p_T in GeV/c). The TPC also provides up to 359 measurements (338 from wires and 21 from pads) of the ionization energy loss allowing electrons to be separated by more than 3σ from the other particle species up to momenta of ~ 8 GeV/c. The TPC is surrounded by the electromagnetic calorimeter (ECAL), which measures the energy of electrons and photons with a resolution $\sigma(E)/E = 0.18/\sqrt{E} + 0.009$ (E in GeV). The arrival time of the signals are also measured by the ECAL with a resolution of ~ 20 ns, thus allowing signals associated with a bunch crossing to be discriminated from signals induced, *e.g.,* by cosmic rays. The return yoke of the magnet, instrumented with streamer tubes, forms the hadron calorimeter (HCAL) which provides a measurement of the energy of charged and neutral hadrons with a resolution

2

$\sigma(E)/E = 0.85/\sqrt{E}$ (E in GeV). The HCAL is surrounded by two double layers of streamer tubes, the muon chambers. Luminosity monitors (LCAL and SICAL) extend the calorimetric coverage down to a polar angle of 34 mrad. The ALEPH triggers relevant for this analysis are based on the total energy deposit in ECAL or on the coincidence between a track candidate in the ITC and an energy deposit in the calorimeter modules to which the track is pointing.

Using the energy flow algorithm described in Ref. [9], the measurements of the tracking detectors and of the calorimeters are combined into "objects" classified as charged particles, photons, and neutral hadrons. The energy resolution achieved with this algorithm is $(0.6\sqrt{E} + 0.6)$ GeV (E in GeV). Electrons are identified by comparing the energy deposit in ECAL to the momentum measured in the tracking system and by using the shower profile in the electromagnetic calorimeter and the measurement of the specific ionization energy loss in the TPC. The identification of muons makes use of the hit pattern in HCAL and of the muon chambers.

3   Monte Carlo simulation

Since the simulation of the hadronization of stop quarks and of the detector response to long lived stop-hadrons is not available in the standard Monte Carlo programs, a dedicated event generator and a detector simulation program have been developed for the present analysis.

The event generator is a modified version of the one described in Ref. [4]. Since the stop lifetime is larger than the typical hadronization time, colourless stop-hadrons $\widetilde{\mathrm{T}}$ are formed. This has been incorporated in the generator by applying to stop quarks the standard Lund string fragmentation scheme as implemented in JETSET 7.4 [10]. A Peterson fragmentation function [11] is used, with a stop fragmentation parameter $\epsilon_{\widetilde{t}}$ scaled from the b-fragmentation parameter according to the relation $\epsilon_{\widetilde{t}} = \epsilon_{\mathrm{b}}(m_{\mathrm{b}}/m_{\widetilde{t}})^2$. (A value of 0.0035 has been taken for ϵ_{b} [12].) The stop hadrons subsequently decay according to a spectator model.

The effective spectator mass M_{eff}, which regulates the mass of the stop-hadrons, is set to $500\,\mathrm{MeV}/c^2$. The resulting stop-hadron mass is found to be typically $300\,\mathrm{MeV}/c^2$ greater than the stop quark mass. Since a reliable prediction of the mass spectrum of the stop-hadrons and of their excited states is not available, all stop-hadrons are assumed to be equal in mass, with an absolute value of the electric charge ≤ 1. Under these assumptions, double neutral ($\widetilde{\mathrm{T}}^0\widetilde{\mathrm{T}}^0$), mixed ($\widetilde{\mathrm{T}}^\pm\widetilde{\mathrm{T}}^0$) or double charged ($\widetilde{\mathrm{T}}^\pm\widetilde{\widetilde{\mathrm{T}}}^\mp$, $\widetilde{\mathrm{T}}^\pm\widetilde{\mathrm{T}}^\pm$) final states are possible. If a final $\widetilde{\mathrm{T}}\widetilde{\mathrm{T}}$ system with non zero total electric charge is produced, charge conservation is ensured by the fragmentation particles. The relative composition of final state stop hadron charge configurations is shown in Fig. 2 as a function of the stop mass for a centre-of-mass energy of $200\,\mathrm{GeV}$. Since the energy available to produce fragmentation particles is smaller at higher masses, the fraction of $\widetilde{\mathrm{T}}\widetilde{\mathrm{T}}$ with non zero total charge decreases in that mass region.

A major issue of the simulation is the treatment of the interaction of stop-hadrons in the detector. The electromagnetic interaction is simulated by treating a stop-hadron as a heavy pion. The simulation of the strong interaction is based on the following considerations. In the scattering of a stop-hadron $\widetilde{\mathrm{T}}$ of energy $E_{\widetilde{\mathrm{T}}}$ with a nucleon N at rest, the available centre-of-mass energy E_{cm} is given by $E_{cm}^2 = M_{\widetilde{\mathrm{T}}}^2 + M_{\mathrm{N}}^2 + 2M_{\mathrm{N}}E_{\widetilde{\mathrm{T}}}$. The generic reaction is
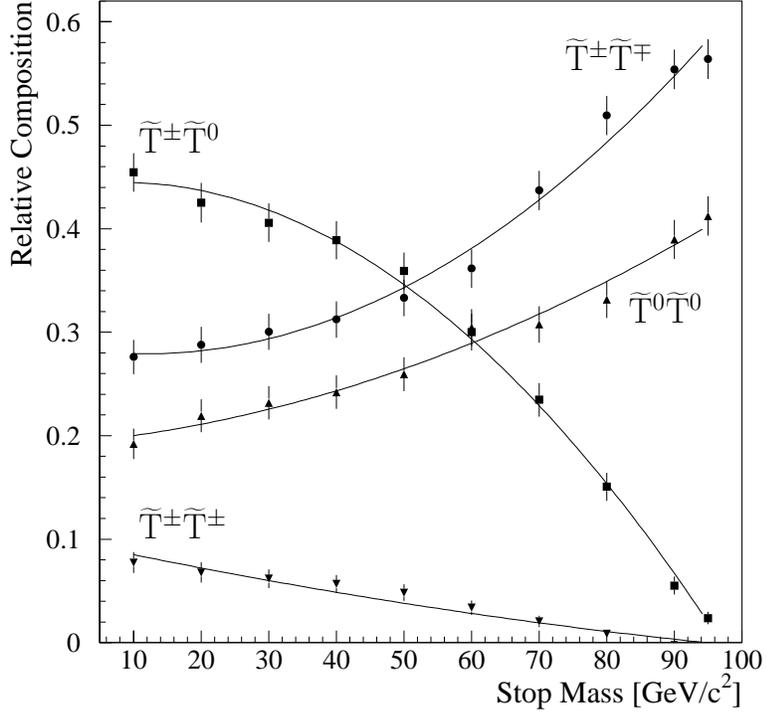
Figure 2: Relative composition of the possible $\widetilde{T}\widetilde{T}$ charge configurations as a function of the stop mass at $\sqrt{s} = 200\,\text{GeV}$.

$\widetilde{T} + N \rightarrow \widetilde{T}' + N' + X$, with a Q-value, which is the maximum energy available for the system X, of $Q = E_{cm} - M_{\widetilde{T}} - M_N$. Since the centre-of mass energy E_{cm} is typically close to $M_{\widetilde{T}}$, only a Q-value of a few hundred MeV is available. For example, for $M_{\widetilde{T}} = 50\,\text{GeV}/c^2$ and $E_{\widetilde{T}} = 90\,\text{GeV}$ the resulting Q-value is $\sim 800\,\text{MeV}$. Therefore, only a few pions may be produced in an inelastic collision, and the stop-hadron behaves in its passage through matter basically like a pion with the corresponding kinetic energy. The routines for the simulation of the stop-hadron strong interaction have thus been derived from the corresponding ones for pions in the GHEISHA [13] hadronic shower simulation package, but with all energy based quantities rescaled to the kinetic energy of the $\widetilde{T}$ hadron, and with the low energy pion nucleon resonances removed.

In order to design the selection criteria, about 500 signal Monte Carlo samples of 1000 events each were generated for various $(m_{\tilde{t}}, m_{\chi})$ combinations, stop lifetimes and centre-of-mass energies, and with a value of $56°$ for $\theta_{\tilde{t}}$. To simulate the relevant Standard Model background processes, several Monte Carlo generators have been used: BHWIDE [14] for Bhabha scattering, KORALZ [15] for $\mu^+\mu^-$ and $\tau^+\tau^-$ production, PHOT02 [16] for $\gamma\gamma$ interactions, KORALW [17] for WW production, and PYTHIA [10] for all other processes. The size of the simulated samples typically corresponds to ten times the integrated luminosity of the data. All background and signal samples were processed through the full detector simulation.

4

4   Analysis

The data sets analysed consist of 173.6 pb^{-1} at 188.6 GeV collected in 1998, and 28.9 pb^{-1} at 191.6 GeV, 79.8 pb^{-1} at 195.5 GeV, 86.3 pb^{-1} at 199.5 GeV and 41.9 pb^{-1} at 201.6 GeV collected in 1999.

The signal final state topology depends strongly on the $\tilde{t}$ decay length $\lambda_{\tilde{t}}$. Three different selections have therefore been used, each designed to cope with a specific $\lambda_{\tilde{t}}$ range. The already existing search for acoplanar jets [4, 5, 6, 7] covers the case of very small lifetimes, while new searches for heavy stable charged hadrons and for tracks with a large impact parameter were specifically designed to address the very large and intermediate lifetime ranges, respectively.

The positions of the most important cuts were determined according to the $\overline{N}_{95}$ prescription [18], *i.e.,* by minimization of the 95% C.L. cross section upper limit expected in the absence of a signal.

4.1   Small lifetimes

If the stop lifetime is negligible, the signature is the one covered by the "low-Δm" acoplanar jet selection detailed in Ref. [4] and updated up to $\sqrt{s} = 202$ GeV in Refs. [5, 6, 7]. The efficiency of that selection as a function of $\lambda_{\tilde{t}}$ is shown in Fig. 3 for $m_{\tilde{t}} = 60$ GeV/c^2 and $\Delta m = 4$ GeV/c^2. Five candidate events were selected in the data, in agreement with the Standard Model background expectation of 3.7 events.

4.2   Intermediate lifetimes

The intermediate lifetime selection addresses the case of stop-hadrons decaying well within the tracking volume, but at a significant distance from the interaction vertex. It is based essentially on the tagging of tracks with a large impact parameter, originating from the stop-hadron decay. Since Δm is small, the heavy neutralino carries away most of the available energy, and the events are therefore characterized by only a few soft charged particle tracks: those from the decay of the charmed hadron formed in the c quark hadronization, and fragmentation tracks from the primary vertex.

Only charged particle tracks with momentum larger than 1 GeV/c are considered. They are divided into two categories:

- PV-tracks coming from the primary vertex, such that $|\cos\theta| < 0.95$, $|d_0| < 0.5$ cm, $|z_0| < 3$ cm, and with at least four TPC hits,

- IP-tracks with a significant impact parameter, such that $|d_0| > 0.5$ cm or $|z_0| > 3$ cm,

where d_0 and z_0 are the transverse and longitudinal track impact parameters, respectively.

At least one IP-track is required. In the following, the quantities pertaining to the highest and second highest energy PV-tracks (IP-tracks) are referred to with the suffixes PV$_i$ (IP$_i$), with $i = 1, 2$, respectively.
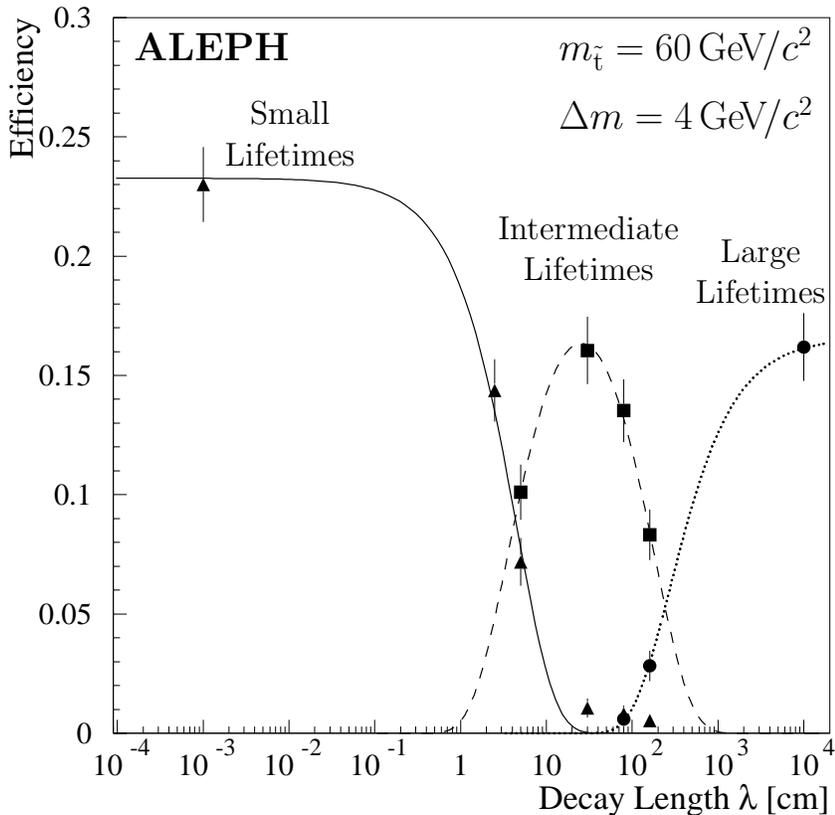
Figure 3: Signal efficiency as a function of the stop decay length at $\sqrt{s} = 200\,\text{GeV}$ for $m_{\tilde{t}} = 60\,\text{GeV}/c^2$ and $\Delta m = 4\,\text{GeV}/c^2$. The three curves correspond to the "low Δm" acoplanar jet selection (solid line) for small lifetimes, the intermediate lifetime selection (dashed line), and the large lifetime selection (dotted line). They are representative of the parametrizations used to derive the final results.

Cosmic muons crossing the detector volume are a major source of charged tracks not originating from the primary vertex. Most of them are rejected by requiring that the ECAL signals be compatible with the beam crossing time within 100 ns. Since cosmic rays are normally reconstructed as two different but collinear tracks, an event is rejected if it contains two IP-tracks such that $|\cos\theta_{IP_1} + \cos\theta_{IP_2}| < 0.02$ or $|\phi_{IP_1} - \phi_{IP_2}| > 178°$.

In Standard Model processes, tracks with large impact parameters can be produced by multiple scattering or nuclear interaction of a primary particle, or by a photon conversion. Because of its huge cross section, $\gamma\gamma$ scattering is the main potential source for this kind of background. The following cuts are designed to reject events from $\gamma\gamma$ interactions, characterized by their small visible energy and by their boost along the beam direction: the visible energy is required to be greater than $2\%\sqrt{s}$; the momenta of the leading and next to leading PV-tracks, if present, are required to exceed $11\%\sqrt{s}$; the polar angle of the missing momentum vector must exceed $53°$; no energy must be detected within $12°$ of the beam axis; the polar angle θ_{IP_1} must be greater than $53°$, and similarly for θ_{PV_1} if there is at least one PV-track.

The large amount of energy carried away by the undetected neutralinos can be *a priori* exploited with a cut on the event visible energy. If however a stop-hadron is charged and

decays at a distance from the primary vertex such that its track is correctly detected and reconstructed, its energy is recorded by the energy flow algorithm, inadequately for the present purpose. The leading or next to leading PV-track is considered a decaying charged stop-hadron candidate if it ends up in a decay vertex or a kink. A corrected visible energy is computed, from which the energy of the decaying charged stop-hadron candidates is excluded, and this corrected visible energy is required to be smaller than $20\%\sqrt{s}$.

The signal topology is further selected by requiring $1\%\sqrt{s} < p_{\mathrm{IP}_1} < 8\%\sqrt{s}$ and $1 \mathrm{~cm} < |d_{0\mathrm{IP}_1}| < 100 \mathrm{~cm}$. Finally, the cut $p_{\mathrm{IP}_1} + p_{\mathrm{IP}_2} > 4\,\mathrm{GeV}/c$ is applied on the sum of the momenta of the two leading IP-tracks, which are expected to originate from charmed hadron decays.

The selection efficiency is shown in Fig. 3 as a function of the decay length for a stop mass of $60\,\mathrm{GeV}/c^2$ and a Δm of $4\,\mathrm{GeV}/c^2$. The background is dominated by the $\gamma\gamma \to q\overline{q}$ and $\gamma\gamma \to \tau^+\tau^-$ processes, and has a total expectation of 0.85 events. No events were selected in the data.

4.3   Large lifetimes

When the stop decay length is larger than the detector size, a charged stop-hadron behaves like a heavy stable charged particle. It can be identified using the kinematic characteristics of stop pair-production and the high specific ionization that it is expected to release in the TPC. The selection criteria are similar to the ones used in Ref. [19]. For a given stop mass hypothesis, at least one stop-hadron track candidate must be found, fulfilling the following requirements: both the reconstructed stop-hadron mass, defined as $M_{\mathrm{rec}} = \sqrt{s/4 - p^2}$, and the specific ionization loss must be compatible with their expectation values, with the exact cuts optimized as a function of the stop mass.

The $\gamma\gamma$ background is eliminated by requiring $p_T > 0.1\sqrt{s}$ for the stop-hadron track candidate. The charged stop-hadron candidate must deposit less than $25\,\mathrm{GeV}$ in ECAL and $10\,\mathrm{GeV}$ in HCAL. These cuts are used to reject Bhabha events, the latter being relevant when electrons enter an ECAL insensitive region. Cosmic ray events are rejected by requiring $|d_0| < 0.3 \mathrm{~cm}$ and $|z_0| < 5 \mathrm{~cm}$.

The cut on the specific ionization does not discriminate between stop-hadron tracks and muon tracks in the stop-hadron mass region around $60\,\mathrm{GeV}/c^2$. In the analysis performed for this stop hadron mass hypothesis, a minimum of two stop-hadron track candidates is required, among which the two leading tracks in the event, and additional cuts are applied to reject radiative dimuons. In contrast to such background events, signal events are expected to contain two nearly back-to-back and equal momentum tracks. It is therefore required that the angle between the directions of the two leading tracks be greater than $178°$, and that their momenta be compatible within three standard deviations.

The selection efficiency is shown in Fig. 3 as a function of the decay length for a stop mass of $60\,\mathrm{GeV}/c^2$. The background is dominated by double radiative dimuon events and has a total expectation of 0.2 events, except in the stop-hadron mass region where the charged stop-hadron ionization loss is similar to the one of a muon. In this mass region a background of 1.0 events is expected. One candidate event was selected in the data at a centre-of-mass energy of $189\,\mathrm{GeV}$,

with two charged tracks compatible with a stop-hadron mass of $\sim 60\,\mathrm{GeV}/c^2$. It is therefore a candidate event in the $\mathrm{d}E/\mathrm{d}x$ overlap region discussed above.

5 Systematic uncertainties

The efficiencies of the intermediate and large lifetime selections may be affected by uncertainties regarding the assumptions on the stop hadron physics and by uncertainties related to the detector response. In the case of the low-Δm acoplanar jet selection, the systematic uncertainty on the efficiency has been evaluated following the procedure described in Ref. [4]. The results of the systematic studies are summarized in Table 1 for the three selections.

The systematic effects from the assumptions on the stop hadron physics have been assessed by varying the parameters of the model implemented in the generator. The uncertainties from the stop hadron mass have been evaluated by varying the effective spectator mass M_{eff}, which has been set to 0.5 GeV/c^2 in the analysis, in the range between 0.3 and 1.0 GeV/c^2. The efficiencies of the intermediate and large lifetime selections have been found to be almost insensitive to this change. The 10% effect found for the low-Δm acoplanar jet selection reflects the variation in the invariant mass available for the hadronic system.

The dependence of the efficiencies on the stop fragmentation has been evaluated by varying the paramater $\epsilon_{\tilde{\mathrm{t}}}$, thereby changing the energy available for the fragmentation particles. A rather drastic variation of $\epsilon_{\tilde{\mathrm{t}}}$ has been considered, allowing it to be decreased by an order of magnitude. The relative amount of the $\widetilde{\mathrm{T}}\widetilde{\mathrm{T}}$ charge configurations depends on the probability to produce fragmentation tracks. Therefore, the variation of $\epsilon_{\tilde{\mathrm{t}}}$ also provides an evaluation of the systematic uncertainty with respect to the $\widetilde{\mathrm{T}}\widetilde{\mathrm{T}}$ charge composition. The mean $\widetilde{\mathrm{T}}\widetilde{\mathrm{T}}$ charge is found to have a relative maximal change of about 20% for the considered $\epsilon_{\tilde{\mathrm{t}}}$ range. The largest relative change in efficiency, about 12%, has been found for the intermediate lifetime selection.

The amount of initial state radiation in stop pair production depends on the value of the stop coupling to the Z boson, which is controlled by the stop mixing angle. A variation of $\theta_{\tilde{\mathrm{t}}}$ from 56° to 0°, *i.e.*, from minimal to maximal coupling, has been applied. For all selections the effect has been found to be small, at the level of 1 to 3%.

Systematic uncertainties (%)			
	Selection		
	Acoplanar Jets low-Δm	Intermediate Lifetimes	Large Lifetimes
M_{eff} (0.3–1.0 GeV)	10	*negl.*	1
$\epsilon_{\tilde{\mathrm{t}}}(\epsilon_{\mathrm{b}} = 0.003 - 0.06)$	2	12	2
$\theta_{\tilde{\mathrm{t}}}$ (0°–56°)	1	1	3
Detector effects	*negl.*	*negl.*	3
Monte Carlo statistics	3	3	3
TOTAL	11	12	6

Table 1: Summary of the relative systematic uncertainties on the $\tilde{\mathrm{t}}$ selection efficiencies.

Detector effects have been studied for the variables used in the analyses. The systematic uncertainties associated with the large lifetime selection cuts based on kinematics have been evaluated using a sample of dimuon events. The performance of the tracking has been checked on a sample selected with criteria independent of those used in the analysis. The performance of the energy loss algorithm has been checked with electrons, muons, and pions, selected by using calorimeter information only. From these studies, a total systematic uncertainty of 3% on the selection efficiency has been estimated.

The impact parameter distribution has been checked on hadronic events collected during the 1999 runs at the Z resonance. The negative part of the distribution (which is not affected by lifetime) shows good agreement with the Monte Carlo expectation.

The beam-related background may affect the $E_{12°}$ variable used in the acoplanar jet and intermediate lifetime selections. This background is not included in the event simulation. Its effect on the selection efficiency has been determined from data collected at random beam crossings. The net effect is a relative decrease of the signal efficiency of about 5%. The systematic uncertainty on this correction is negligible.

Finally, an additional uncertainty of 3% due to the limited Monte Carlo statistics has been added. The total systematic uncertainties have been found to be at the level of 11 and 12% for the low-Δm acoplanar jet and for the intermediate lifetime selections, respectively. In both cases they are dominated by the limited knowledge of the stop hadron physics and result from rather extreme changes in the model parameters. The systematic uncertainty for the large lifetime selection is at the level of 6%.

6 Results

Since no excess of candidate events was observed, lower limits on the stop mass have been set. The systematic uncertainties on the selection efficiencies have been included as suggested in Ref. [20], and no background subtraction has been performed. The efficiencies and backgrounds have been parametrized as a function of $m_{\tilde{t}}$, Δm and of the stop-hadron proper decay length $c\tau_{\tilde{t}}$ ($\lambda_{\tilde{t}} = (p_{\tilde{t}}/m_{\tilde{t}})c\tau_{\tilde{t}}$) . For each value of $m_{\tilde{t}}$, Δm and $c\tau_{\tilde{t}}$, all logical combinations of the available selections have been considered, and the best combination was chosen according to the $\overline{N}_{95}$ prescription.

The lower limit on the stop mass is shown in Fig. 4a as a function of $\log(c\tau_{\tilde{t}}/cm)$ for various Δm values, and in Fig. 4b as a function of Δm for various $\log(c\tau_{\tilde{t}}/cm)$. The smallest Δm value considered is 1.6 GeV/c^2, corresponding to $m_D - 300$ MeV/c^2, *i.e.,* the kinematic limit for the decay $\tilde{t} \to c\chi$ for $M_{eff} = 500$ MeV/c^2, and with the D-meson mass $m_D \sim 1.9$ GeV/c^2. Below that Δm value, the stop decay mode is $\tilde{t} \to u\chi$, and the limit is given by the search for heavy stable stop-hadrons. The absolute mass lower limit obtained is 59 GeV/c^2. It is reached for $\Delta m = 1.6$ GeV/c^2 and for a $c\tau_{\tilde{t}}$ value of ~ 1 cm. In that configuration of parameters, the acoplanar jet and intermediate lifetime selections are combined. The limit on $m_{\tilde{t}}$ does not depend on the choice made for M_{eff}; only the Δm value for which it is reached does, through the value of the stop-hadron mass ($\Delta m = m_D - (m_{\tilde{T}} - m_{\tilde{t}})$).
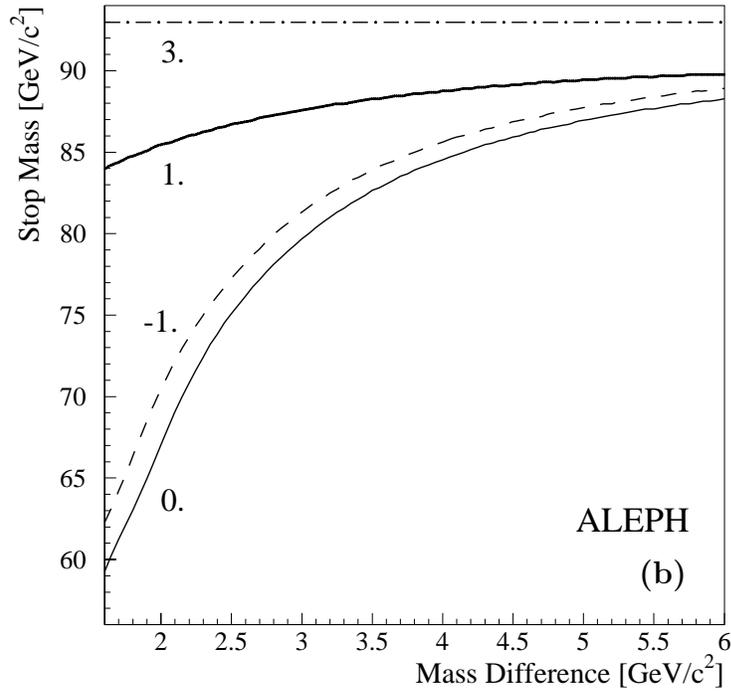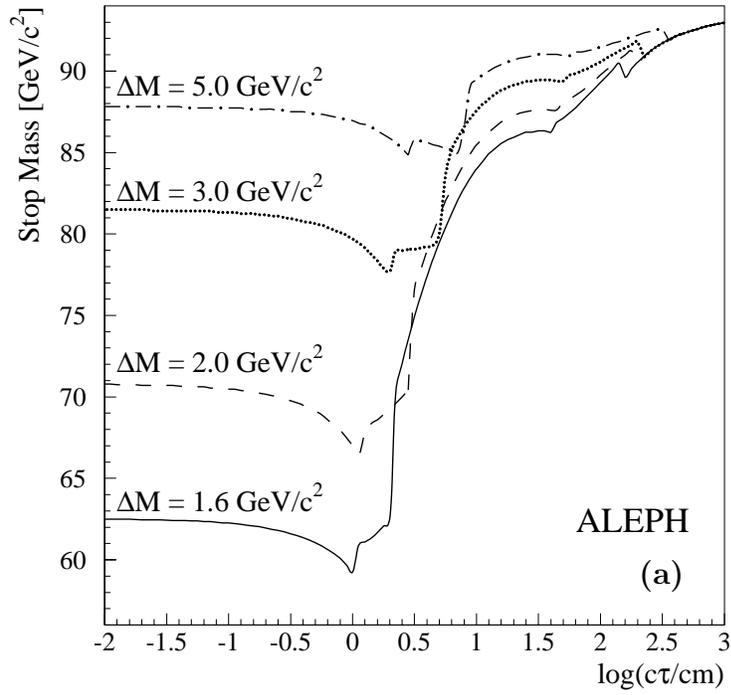
Figure 4: Stop mass 95% C.L. lower limit as a function of $\log(c\tau_{\tilde{t}}/\text{cm})$ for several Δm values (a), and as a function of Δm for several $\log(c\tau_{\tilde{t}}/\text{cm})$ values (b).

The stop mass lower limit can be tightened in the MSSM if the theoretical relation [3] between the decay width and Δm is used. For instance, the 95% C.L. excluded region in the plane $(m_{\tilde{t}}, \Delta m)$, obtained for $\theta_{\tilde{t}} = 56°$, $\mu = -100\,\mathrm{GeV}$ and $\tan\beta = 1.5$, is shown in Fig. 5a. The regions excluded by the single analyses are also shown. In order to set an absolute lower limit on the stop mass, a scan over the relevant MSSM parameters has been performed. The limit as a function of $\tan\beta$, obtained by scanning over Δm, μ and $\theta_{\tilde{t}}$, is shown in Fig. 5b. The absolute 95% C.L. lower limit on $m_{\tilde{t}}$ is 63 GeV/c^2. It is set for $\Delta m = 1.9\,\mathrm{GeV}/c^2$, $\tan\beta = 2.6$, $\theta_{\tilde{t}} = 56°$, and for large negative μ.

7   Conclusions

Searches for signals from pair production of the scalar top have been performed in the data sample of 411 pb^{-1} collected in 1998 and 1999 by the ALEPH detector at LEP, at centre-of-mass energies from 188.6 to 201.6 GeV. The searches are dedicated to the decay channels $\tilde{t} \to c\chi$ and $\tilde{t} \to u\chi$, in the regime where the mass difference Δm between the stop and the neutralino is small, and where the stop could have a sizeable lifetime. In all cases, the numbers of candidates observed are found to be consistent with the background expected from Standard Model processes. In the MSSM, and assuming no additional source of flavour changing neutral currents with respect to the Standard Model, a 95% C.L. lower limit of 63 GeV/c^2 is obtained for the stop mass, valid for any value of Δm. If the MSSM theoretical relation between Δm and the stop lifetime is ignored, this lower limit becomes 59 GeV/c^2.
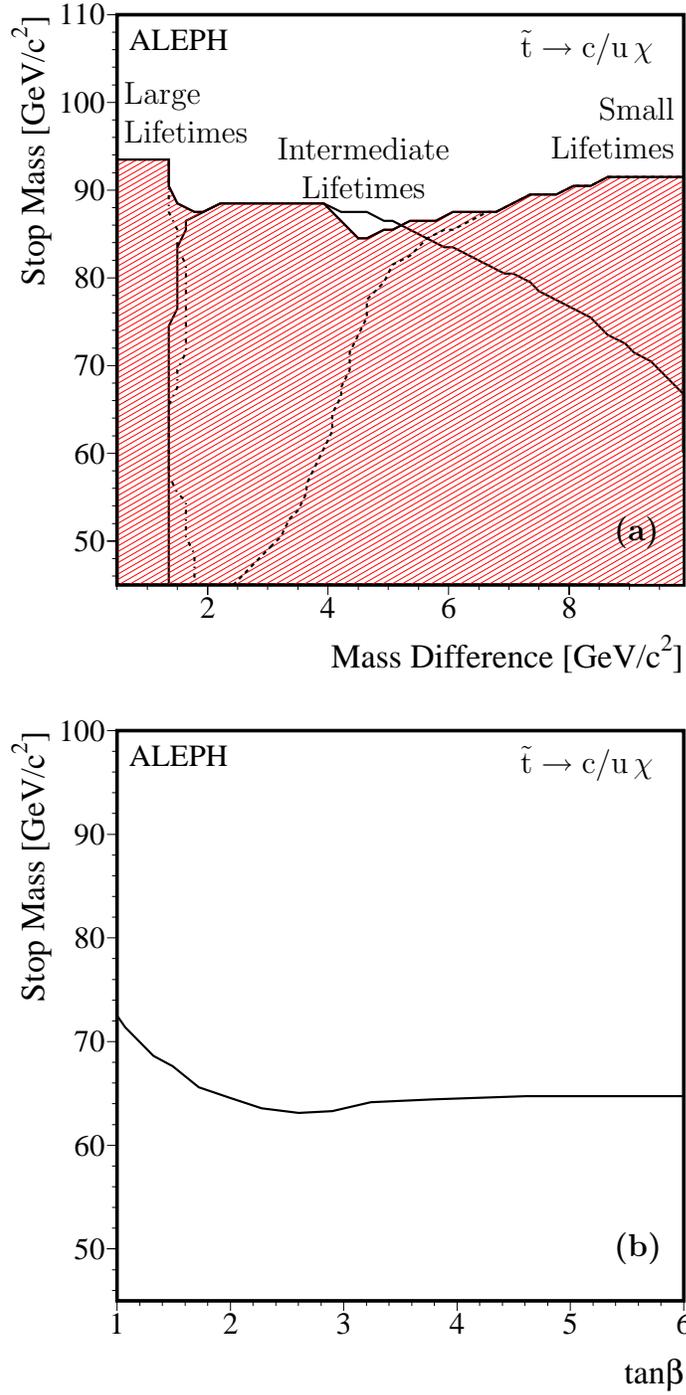
Acknowledgements

Figure 5: In the MSSM: (a) 95% C.L. excluded region in the plane $m_{\tilde{t}}$ *vs.* Δm, for $\theta_{\tilde{t}} = 56°$, $\mu = -100$ GeV, and $\tan\beta = 1.5$, where the hatched area is the region excluded by the optimal combination of the used selections and the lines are the limits from each selection used independently; (b) stop mass 95% C.L. lower limit as a function of $\tan\beta$, independent of Δm, μ and $\theta_{\tilde{t}}$.

12

References

[1] J. Ellis and S. Rudaz, *Search for supersymmetry in toponium decays*, Phys. Lett. **B 128** (1983) 248.

[2] M. Drees and K. Hikasa, *Scalar Top production in* e$^+$e$^-$ *annihilation*, Phys. Lett. **B 252** (1990) 127.

[3] K. Hikasa and M. Kobayashi, *Light Scalar Top at* e$^+$e$^-$ *colliders*, Phys. Rev. **D 36** (1987) 724.

[4] ALEPH Collaboration, *Searches for Scalar Top and Scalar Bottom Quarks at LEP2*, Phys. Lett. **B 413** (1997) 431.

[5] ALEPH Collaboration, *Scalar quark searches in* e$^+$e$^-$ *collisions at* $\sqrt{s} = 181 - 184\,\text{GeV}$, Phys. Lett. **B 434** (1998) 189.

[6] ALEPH Collaboration, *Searches for sleptons and squarks in* e$^+$e$^-$ *collisions at* 189 GeV, Phys. Lett. **B 469** (1999) 303.

[7] ALEPH Collaboration, *Search for Sfermions, Charginos and Neutralinos in* e$^+$e$^-$ *Collisions at* $\sqrt{s}$ *up to* 201.6 GeV *and Mass Limit on the Lightest Neutralino*, ALEPH-CONF 2000-009.

[8] ALEPH Collaboration, *ALEPH: A Detector for Electron - Positron annihilations at LEP*, Nucl. Instrum. and Methods **A 294** (1990) 121.

[9] ALEPH Collaboration, *Performance of the ALEPH detector at LEP*, Nucl. Instrum. and Methods **A 360** (1995) 481.

[10] T. Sjöstrand, *High-energy-physics event generation with* `PYTHIA 5.7` *and* `JETSET 7.4`, Comput. Phys. Commun. **82** (1994) 74.

[11] C. Peterson, D. Schlatter, I. Schmitt and P.M. Zerwas, *Scaling violations in inclusive* e$^+$e$^-$ *annihilation spectra*, Phys. Rev. **D 27** (1983) 105.

[12] ALEPH Collaboration, *Studies of Quantum Chromodynamics with the ALEPH Detector*, Physics Reports **294** (1998) 1.

[13] H.C. Fesefeldt, *The simulation of hadronic showers: physics and applications*, PITHA/85-02 (1985).

[14] S. Jadach, W. Placzek and B. F. Ward, `BHWIDE 1.00`: $\mathcal{O}(\alpha)$ *YFS exponentiated Monte Carlo for Bhabha scattering at wide angles for LEP1/SLC and LEP2*, Phys. Lett. **B 390** (1997) 298.

[15] S. Jadach, B. F. Ward and Z. Was, *The Monte Carlo program* `KORALZ`, *version 4.0, for the lepton or quark pair production at LEP/SLC energies*, Comput. Phys. Commun. **79** (1994) 503.

[16] J.A.M. Vermaseren, *Two Gamma Physics Versus One Gamma Physics And Whatever Lies In Between*, in *Proceedings of the IVth international Workshop on Gamma Gamma Interactions*, Eds. G. Cochard and P. Kessler, Springer Verlag, 1980;
ALEPH Collaboration, *An experimental study of* $\gamma\gamma \rightarrow$ hadrons *at LEP*, Phys. Lett. **B 313** (1993) 509.

[17] S. Jadach, W. Placzek, M. Skrzypek, B. F. Ward and Z. Was, *Monte Carlo program* `KORALW 1.42` *for all four-fermion final states in* e^+e^- *collisions*, Comput. Phys. Commun. **119** (1999) 272.

[18] ALEPH Collaboration, *Search for the Standard Model Higgs Boson*, Phys. Lett. **B 313** (1993) 299;
J.F. Grivaz, F. Le Diberder, *Complementary analyses and acceptance optimization in new particle searches*, LAL **92-37** (1992).

[19] ALEPH Collaboration, *Search for Gauge Mediated SUSY Breaking Topologies at* $\sqrt{s} \sim 189 \, \text{GeV}$, CERN EP/99-171 (submitted to Eur. Phys. J.).

[20] R.D. Cousins, V.L. Highland, *Incorporating systematic uncertainties into an upper limit*, Nucl. Instrum. and Methods **A 320** (1992) 331.